Water Research 219 (2022) 118597

Contents lists available at ScienceDirect

Water Research

journal homepage: www.elsevier.com/locate/watres

High-rate microbial electrosynthesis using a zero-gap flow cell and vapor-fed anode design

Gahyun Baek [a,b], Ruggero Rossi [a], Pascal E. Saikaly [c,d], Bruce E. Logan [a,*]

[a] Department of Civil and Environmental Engineering, Penn State University, 231Q Sackett Building, University Park, PA 16802, United States
[b] Environmental Research Group, Research Institute of Industrial Science and Technology (RIST), 67 Cheongam-ro, Nam-gu, Pohang-si, Gyeongsangbuk-do, 37673 Republic of Korea
[c] Environmental Science and Engineering Program, Biological and Environmental Science and Engineering Division, King Abdullah University of Science and Technology, Thuwal 23955-6900, Saudi Arabia
[d] Water Desalination and Reuse Center, King Abdullah University of Science and Technology, Saudi Arabia

ARTICLE INFO

Keywords:
Microbial electrosynthesis
Carbon capture and utilization
Zero-gap electrode design
Vapor-fed anode

ABSTRACT

Microbial electrosynthesis (MES) cells use renewable energy to convert carbon dioxide into valuable chemical products such as methane and acetate, but chemical production rates are low and pH changes can adversely impact biocathodes. To overcome these limitations, an MES reactor was designed with a zero-gap electrode configuration with a cation exchange membrane (CEM) to achieve a low internal resistance, and a vapor-fed electrode to minimize pH changes. Liquid catholyte was pumped through a carbon felt cathode inoculated with anaerobic digester sludge, with humidified N_2 gas flowing over the abiotic anode (Ti or C with a Pt catalyst) to drive water splitting. The ohmic resistance was 2.4 ± 0.5 mΩ m^2, substantially lower than previous bioelectrochemical systems (20–25 mΩ m^2), and the catholyte pH remained near-neutral (6.6–7.2). The MES produced a high methane production rate of 2.9 ± 1.2 L/L-d (748 mmol/m^2-d, 17.4 A/m^2; Ti/Pt anode) at a relatively low applied voltage of 3.1 V. In addition, acetate was produced at a rate of 940 ± 250 mmol/m^2-d with 180 ± 30 mmol/m^2-d for propionate. The biocathode microbial community was dominated by the methanogens of the genus *Methanobrevibacter*, and the acetogen of the genus *Clostridium sensu stricto 1*. These results demonstrate the utility of this zero-gap cell and vapor-fed anode design for increasing rates of methane and chemical production in MES.

1. Introduction

Carbon dioxide, a major greenhouse gas, can be converted to valuable gaseous or liquid chemical products either using inorganic catalysts in abiotic reactors, or using certain microorganisms in microbial electrosynthesis (MES) cells (Jourdin and Burdyny, 2021; Wood et al., 2021). MES is a nascent bioelectrochemical approach that has been used to convert CO_2 in the cathode chamber into methane gas or chemicals such as acetate, propionate, and other volatile fatty acids, depending on the inoculum and operating conditions (Jiang et al., 2019b; Li et al., 2018). The reduction of CO_2 can occur via direct extracellular electron transfer (EET) by electrotrophic microorganisms using electrons obtained from the cathode or indirectly via abiotic or biocatalyzed H_2 gas production (Bajracharya et al., 2017; Karthikeyan et al., 2019), or through biochemical synthesis using enzymes produced by microorganisms (Lienemann et al., 2018). The MES systems also can be applied to upgrade biogas produced from anaerobic digesters to higher methane content (Liu et al., 2021). The MES platform has several advantages over abiotic electrosynthesis owing to higher selectivity of final products and versatility of microorganisms compared to metal catalysts as well as the renewable nature of biocatalysts due to cell growth (Rabaey and Rozendal, 2010). When methane is the only desired product of MES it is often referred to as a microbial methanogenesis cell (MMC) (Logan et al., 2015). The production of biomethane from renewable electricity sources such as wind and solar is of great interest as the gas can be used without net CO_2 emissions locally or transported for use in natural gas pipelines.

One challenge for methane generation using MES is that production rates and current densities have been relatively low (Prévoteau et al., 2020). One approach to increase rates has been to use various cathode

* Corresponding author.
E-mail address: blogan@psu.edu (B.E. Logan).

https://doi.org/10.1016/j.watres.2022.118597
Received 10 March 2022; Received in revised form 8 May 2022; Accepted 12 May 2022
Available online 13 May 2022

treatments or pure cultures of microorganisms. For example, non-precious metal catalysts have been added to the cathode such as titanium oxide, rhodium, copper, zinc, and nickel (Alqahtani et al., 2018; Baek et al., 2022; S. Das et al., 2021; Jiang et al., 2019a; Siegert et al., 2014). Using Pt on the cathode can increase current densities relative to other metals at the same input energy due to the generation of H_2 (Siegert et al., 2014), but the use of precious metals may not be economically feasible or desirable. Pure cultures have also been used in MES cells and MMCs, for example, using different methanogens to obtain only methane (Beese-Vasbender et al., 2015; Kracke et al., 2020; Mayer et al., 2019) or acetogens to produce volatile fatty acids (VFAs) (Aryal et al., 2017; Batlle-Vilanova et al., 2016; Deutzmann and Spormann, 2017). To maximize current production, very high voltages (> 5.0 V) are often applied to the circuit, yielding low energy efficiencies (< 40%), defined as the electrical energy input into the system compared to the energy in the chemical product. (Zhou et al., 2021, 2020).

Improving the energy efficiency of methane production in MES requires electrochemical cells with low internal resistance. Many MES and MMC tests have been conducted using two-bottle reactors connected by sidearms (Baek et al., 2022; Kracke et al., 2020, 2019; Rojas et al., 2018b; Siegert et al., 2014). This type of system has a very large internal resistance due to the large distances between the electrodes and the narrow cross-sectional area of the sidearm (Rossi and Logan, 2020). Reactors with closely spaced electrodes and the same cross-sectional area for the electrodes and membrane between the electrodes, which is used to avoid gas crossover between the electrodes, can reduce ohmic resistances and thus enable higher current densities at lower applied voltages (Lavender et al., 2022). A major challenge when using an ion exchange membrane between the electrodes is that this can lead to large pH changes in the solution due to preferential transport of salt ions rather than H^+ produced at the anode or OH^- released from water dissociation at the cathode (Rozendal et al., 2006). If a cation exchange membrane (CEM) is used then Na^+ will be transported through the CEM instead of H^+, resulting in acidification of the anode and basification of the cathode due to the accumulation of OH^- ions. An increased catholyte pH will adversely impact methanogens because they have a quite narrow optimal pH range (6.5–7.8) (Fang et al., 2014). In several MES systems, pH has been manually controlled by supplementing the catholyte with a strong acid (Liu et al., 2017; Rojas et al., 2018b; van Eerten-Jansen et al., 2015) or by using a specialized direct CO_2 delivery system using electrocatalytic conductive membranes needed to buffer the pH at the cathode surface (Bian et al., 2021). Otherwise, the catholyte pH will increase to be in the range of 7.7–10.1 depending on the current density (Zhou et al., 2021, 2020).

It was recently shown that performance of microbial fuel cells (MFCs) used to produce electricity and microbial electrolysis cells (MECs) for H_2 production could be improved and pH changes could be mitigated using a combination of closely spaced electrodes, an anion exchange membrane (AEM), and a vapor fed cell (Rossi et al., 2021a, 2021b). In the MECs, the electrodes were placed in contact with the AEM (zero-gap electrode design) to reduce internal resistance and diminish the distance between where H^+ and OH^- ions are produced and consumed, to minimize the development of concentration gradient in the cell. A buffered medium was pumped through the anode chamber to supply substrate for the exoelectrogenic biofilm. No liquid was used for the cathode, and instead a humidified gas was pumped through a cathode chamber to collect hydrogen gas and provide additional water needed for the hydrogen evolution reaction. The lack of a liquid catholyte enhanced effective OH^- transport from the cathode to the anode, resulting in minimal pH changes in the anolyte (Rossi et al., 2021b).

In this study, we examined the use of a zero-gap reactor configuration modified from previous designs to accommodate an electrotrophic cathode biofilm. In this reactor the anode chamber was designed to have a vapor gas feed enabling oxygen evolution at the anode, with a liquid catholyte fed to the biocathode. Instead of using an AEM, as done in an MEC to enable OH^- ion transport to the anode, a CEM was used to facilitate H^+ transport from the anode to the cathode to maintain near-neutral catholyte pH. Unlike previous MECs where H_2 was produced at the vapor-fed cathode under abiotic conditions, this MES configuration results in H_2 generation in the same chamber (i.e., cathode chamber) as the microorganisms. This configuration provided selective enrichment for the growth of microorganisms that either use current directly from the cathode or chemical products evolved from the cathode. In both cases the microbes must remain firmly attached to the electrode in the presence of methane gas generation and transport through the electrode. The inoculation using a mixed anaerobic culture from a digester enabled the possibility of generation of methane as well as other chemicals such as formate, acetate, and other VFAs, in addition to hydrogen gas. To work towards more optimal operating conditions for methane generation, we explored different applied voltages and anode materials and examined their impact on current densities and stability over time.

2. Materials and methods

2.1. MES reactor construction

Duplicate two chambered MES reactors were constructed based on previous zero-gap configurations (Rossi et al., 2021b) but with modifications. The anodes were either carbon cloth (Fuel Cell Store) coated with Pt/C or platinized titanium felt (0.2–0.3 mm thick, porosity of 53–56%, Fuel Cell Store, product code 592,800). A platinum catalyst was added onto the carbon cloth by spraying a mixture of Pt/C and Nafion binder in isopropanol/water onto the cloth using an air brush, with a final Pt loading of 2 mg/cm^2 and Nafion binder loading of 2 mg/cm^2. Platinum was used as the anode catalyst for convenience and cost considerations, although iridium oxide is usually a preferred catalyst for the oxygen evolution reaction. The cathode was carbon felt (3.18 mm of thickness; 0.6 m^2/g of surface area; Alfa-Aesar), and the CEM was Nafion 117 (Fuel Cell Store). All electrodes and the membrane had an exposed projected surface area of 7 cm^2 (used to normalize the gas production rate based on the surface area).

To make a membrane-electrode assembly (MEA), Pt/C on carbon cloth (or platinized Ti felt) was hot pressed (130 °C) at 3000 psi for 2 min to the CEM. The reactors were assembled using plastic end plates, rubber gaskets, a current collector (titanium foil), and plastic spacers. The plastic spacers were inserted between the end plate and the anode to achieve a close contact between MEA and the cathode as well as to allow gas flow past to the anode (Fig. S1). The anode and cathode chambers had a thickness of 3.18 mm due to the width of the gaskets, producing empty volume for both electrode chambers of 4.5 mL (used to normalize the gas production rate), generating 158 m^2/m^3 of surface area-to-volume ratio (Rossi et al., 2021b). The cathode chamber was completely occupied by the carbon felt cathode, thus driving the liquid catholyte flow through the cathode.

2.2. Biocathode acclimation and MES reactor operation

A biocathode was acclimated in single-chamber MECs prior to transferring to MES reactors as previously described (Ragab et al., 2019). The electrodes were first inoculated by amending the medium with effluent from lab-scale MFCs (50% v/v) and anaerobic digester sludge from the Pennsylvania State University wastewater treatment plant (1% v/v) to provide sources for both exoelectrogenic bacteria and hydrogenotrophic methanogens. The medium (pH = 7.0) contained $NaHCO_3$ (2.5 g/L), NH_4Cl (1.5 g/L), NaH_2PO_4 (0.6 g/L), KCl (0.1 g/L), vitamin (10 mL/L), mineral solution (10 mL/L) and sodium acetate (2 g/L as organic source). The headspace and medium were sparged with CO_2/N_2 (20:80 v/v) gas for 10 min before every new cycle and 0.8 V of fixed voltage was applied between the anode and cathode using a potentiostat (VMP2, BioLogic, Knoxville, TN). Carbon felt was heated at 450 °C for 30 min and used for the cathode, and a carbon brush was used as the anode. The biocathodes were acclimated for multiple fed-batch

cycles in the MECs until the methane content of the biogas exceeded that of the hydrogen (> 20 cycles).

The acclimated biocathodes were transferred to MES reactors (abiotic anode) and fed with same electrolyte used for acclimation but without sodium acetate. The catholyte was recirculated from the storage bottle (500 mL) to the cathode at a flow speed of 2.5 mL/min (Fig. 1). The medium in the bottle was completely replaced after each cycle, and it was sparged with CO_2/N_2 (20:80 v/v) gas for 10 min prior to use. The anode was fed with humidified gas (2.5 mL/min) from the headspace of the anode storage bottle filled with deionized water (500 mL) and sparged with 100% N_2 gas. The anode inlet bottle was connected to the gasbag filled with 100% N_2 gas to vent gas from the anode chamber produced by the oxygen evolution reaction, and therefore to reduce oxygen intrusion into the cathode chamber (Fig. 1C). Each batch cycle lasted 2 days except for: the first cycle, set at 5 days to provide a sufficient time for biocathode acclimation; and the last cycle set at 6 days to test the impact of long-term operation on catholyte pH. The biogas was collected from the headspace of catholyte storage bottle and analyzed for gas concentrations.

All experiments were conducted at 30 °C in the dark in duplicate. A fixed voltage between anode and cathode (2.0–3.1 V) was applied and the current produced was recorded every 5 min using potentiostat (VMP2, BioLogic, Knoxville, TN). Unfortunately, the anode and cathode potentials could not be monitored because this reactor design did not have space to insert a reference electrode. The cathode chamber was fully filled with carbon felt and there was no electrolyte in the anode chamber.

2.3. Chemical analyses and calculations

Methane (Q_{CH4}) and hydrogen (Q_{H2}) production rates were calculated based on the biogas composition measured using a gas chromatograph (GC) and total batch cycle time. Biogas from the headspace of catholyte storage bottles was extracted using an airtight gas syringe (Hamilton, Reno, NV, USA) and analyzed using a GC (model 2601B, SRI Instrument, Torrance, CA, USA) equipped with a 3-m Molsieve 5A 80/100 column (Altech Associates, Inc., Bannockburn, IL) and thermal conductivity detector (TCD) with argon as the carrier gas. For liquid chemical analysis, catholyte collected from the recirculation bottle was filtered by using a syringe filter (0.45 μm of pore size). VFAs (formate, acetate, propionate, and butyrate) were measured using high performance liquid chromatography (HPLC; CTO-20A UFLC; Shimadzu, Columbia, MD) equipped with an autosampler (model SIL-20A HT, Shimadzu, Columbia, MD) and column (250 × 4.6 mm, Allure Organic Acids column, 5 μm particle size; Restek, Bellefonte, PA). The current interrupt method was used to estimate the ohmic resistance of MES reactors. The current of 4.5 mA (chosen because this was the average value of two MES reactors in the last cycle during startup) was applied for 2 s and turned to open circuit voltage (OCV) for 2 s. This cycle was repeated 10 times with collecting data every dE = 1.0 mV using a potentiostat (VMP2, BioLogic, Knoxville, TN).

The cathodic recovery (r_{cat}) was calculated as Q_{chem}/Q_i, where Q_{chem} is the coulombs in the recovered chemicals (hydrogen, methane, and VFAs) and Q_i is the total coulombs based on the generated current over one batch cycle.

2.4. Microbial community analysis of cathode biofilm

The cathode biofilm samples were collected at the end of the experiment. The whole cathode was taken out from the reactor and cut into two pieces using sterile scissors. Each sample was stored in the RNA*later*™ stabilization solution (AM7020, ThermoFisher Scientific) overnight to stabilize RNA during shipping of the samples for RNA extraction and sequencing. RNA was extracted using the standard

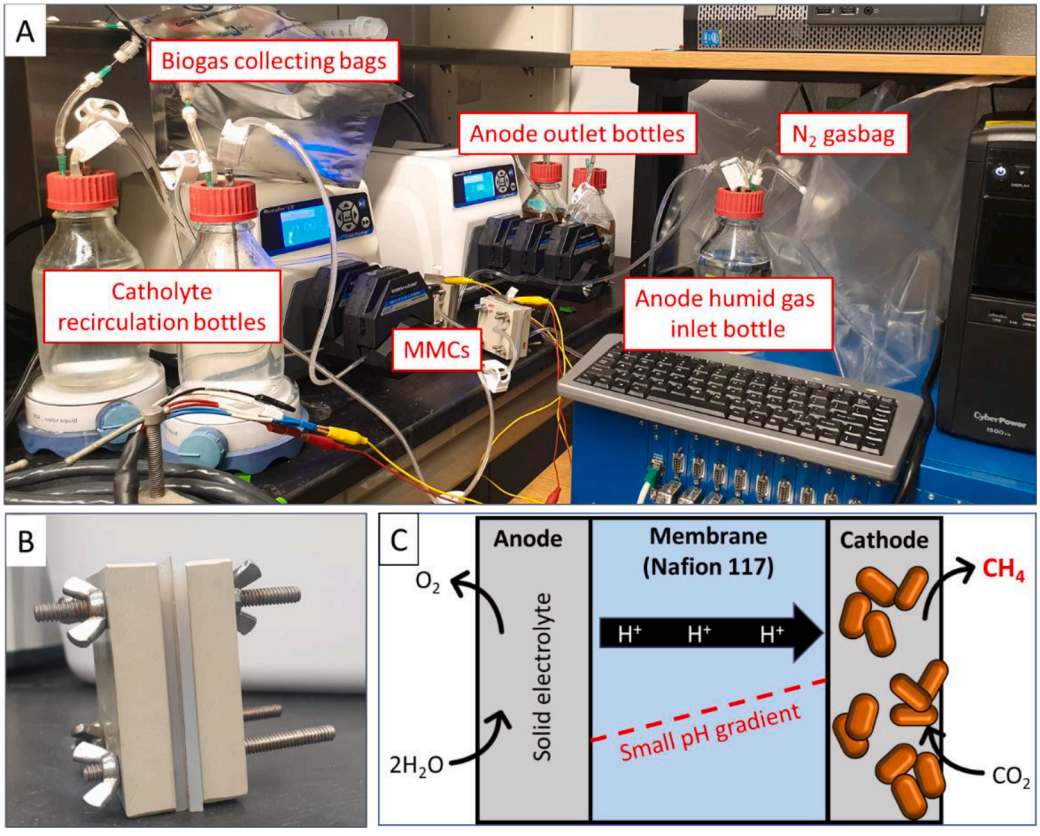

Fig. 1. (A) Photographs of the MES system operation, (B) two-chamber MES system design, and (C) schematics of (bio)electrochemical reactions taking place at the anode and cathode.

protocol for RNeasy PowerMicrobiome Kit (Qiagen, Germany) and reverse-transcribed using 2× Platinum SuperFi RT-PCR Master Mix from the SuperScript IV One-Step RT-PCR System (Thermo Fisher Scientific, USA). The 16S rRNA sequencing libraries were constructed according to the Illumina protocol by using the forward (515F) and reverse (806R) tailed primers. The detailed procedures to perform sequencing and data processing are described in the previous work (Baek et al., 2021).

3. Results & discussion

3.1. Biogas production from MES systems

The initial methane production rate using the carbon anode reached a maximum of 0.4 L/L-d in the second cycle (1.4 A/m^2, E_{ap} = 2.0 V) but declined to 0.1 L/L-d (0.5 A/m^2) by cycle 7 (Fig. 2A). The production rates were similar to several previous MES experiments showing rates of 0.2–0.5 L/L-d (Jiang et al., 2013; Liu et al., 2017; van Eerten-Jansen et al., 2015). However, MES operation clearly resulted in oxidation of the carbon anode, as shown by production of a dark colored liquid from the anode chamber (Fig. S2). Oxidation of carbon-based anodes material has been noted in other MES systems using a set cathode potential of –0.9 V (vs. Ag/AgCl) (Baek et al., 2022). Although the anodic potential could not be monitored in this configuration, a carbon electrode is known to be oxidized at lower anodic potential in the acidic than neutral condition (Yi et al., 2017). The moisture on the carbon anode might be acidic due to a continuous operation, providing a favorable condition for carbon oxidation. To confirm that the decrease in performance over time was due to the anode, the anode was replaced with a new Pt/C carbon cloth in cycle 8 (Fig. 2A). The methane production rate was immediately restored to 0.5 L/L-d, but performance again subsequently decreased until cycle 11 (Q_{CH4} = 0.3 L/L-d) as a result of electrode oxidation.

The performance of the MES stabilized when the carbon cloth anodes were replaced with the platinized titanium felt, and the applied voltage was increased to 2.5 V. The titanium was stable for water splitting consistent with results of several other MES systems using this material (van Eerten-Jansen et al., 2015; Zhou et al., 2021). The slightly higher applied voltage of E_{ap} = 2.5 V did not appreciably increase methane production during cycles 14–16, averaging Q_{CH4} of 0.5 ± 0.0 L/L-d with a current density of 1.9 ± 0.0 A/m^2. Increasing the applied voltage to E_{ap} = 2.8 V for cycles 17–19 significantly improved the methane

	Phase 1	Phase 2	Phase 3	Phase 4	Phase 5	Phase 6
Duration (cycles)	1–7	8–11	12–16	17–19	20–22	23-25
Anode material	CC/Pt	CC/Pt (new)	Ti/Pt	Ti/Pt	Ti/Pt	Ti/Pt
E_{ap} (V)	2.0	2.0	2.5	2.8	3.1	2.8

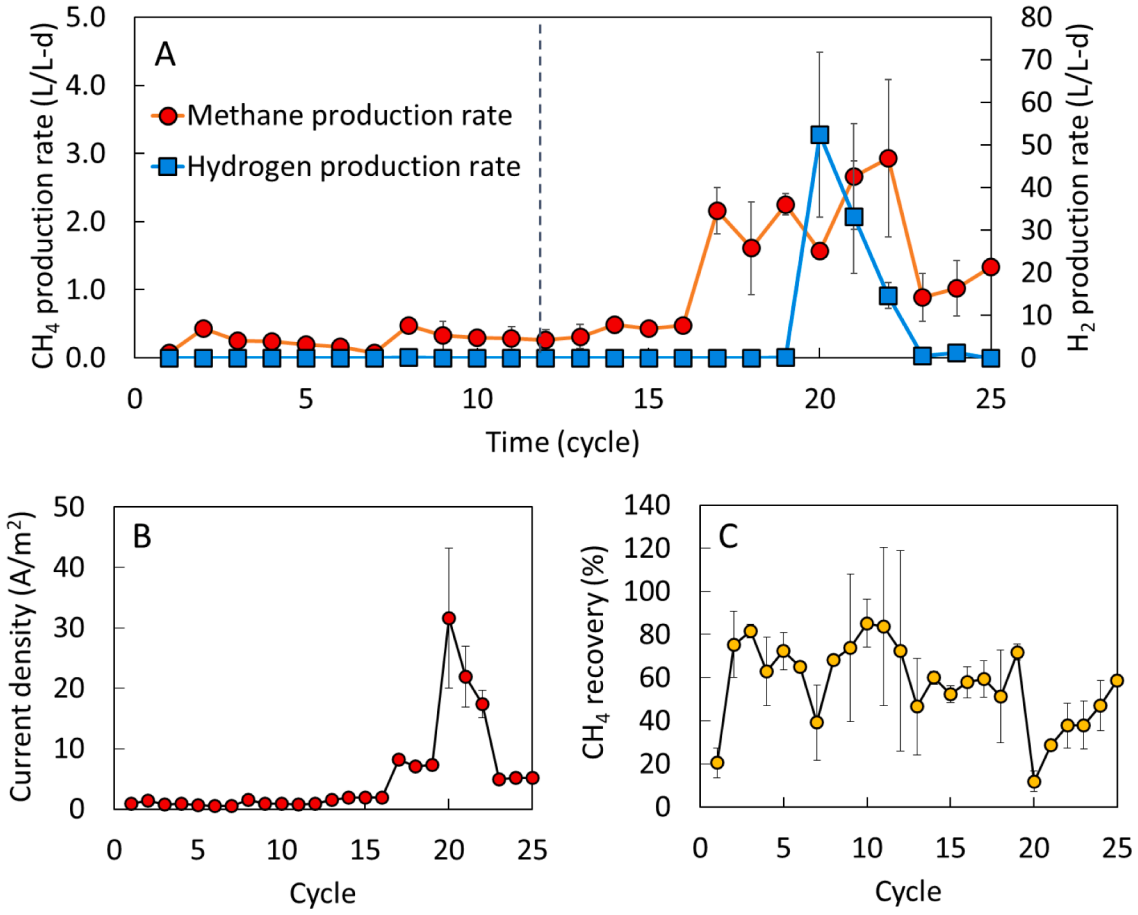

Fig. 2. (A) Methane and hydrogen production rate from MES systems over 25 repeated cycles and changes in operating conditions in each phase. A dotted line indicates the point where the anode material was changed. (B) The average current densities produced and (C) cathodic methane recovery throughout the experiment.

production rate to Q_{CH4} of 2.0 ± 0.3 L/L-d, and current density to 7.5 ± 0.6 A/m^2 (Fig. 2).

When the E_{ap} was further increased to 3.1 V during cycles 20–22, there was no appreciable increase in the rate of methane production (Q_{CH4} = 2.4 ± 0.7 L/L/d during cycles 20–22) (Fig. 2A) despite a 3.1× increase in the current density to 23.6 ± 7.3 A/m^2 (Fig. 2B and Fig. S3). The percentage of methane recovery relative to the current production therefore decreased from 72 ± 4% in cycle 19 to 12 ± 5% in cycle 20 (Fig. 2C). The production of a higher current without an increase in methane resulted in the production of other products, especially H_2 gas at a rate of 52 ± 19 L/L-d (at cycle 20). This high production rate of H_2 indicated that it was being produced faster than it could be consumed by methanogens or other microorganisms on the cathode (Werner et al., 2016).

When the applied voltage was reduced back to an E_{ap} = 2.8 V in cycles 24–27, the methane production rate (1.1 ± 0.2 L/L-d) averaged only 54% of its rate in the previous cycles at this same applied voltage. This reduction in performance suggested that the cathodic biofilm was damaged by the high H_2 gas production rates. A high H_2 gas bubbling rate from the cathode has been used as a means of self-cleaning the surface of a membrane in the membrane bioreactor to reduce biofouling (Katuri et al., 2014). Here, vigorous H_2 evolution could adversely impact MES performance by detaching the microorganisms and the extracellular polymeric matrix that form a biofilm on the electrode surfaces (Dargahi et al., 2014). In addition, low methane production rate could be due to that other microbial groups such as acidogens became dominant at high H_2 production rate, which will be discussed in later section.

3.2. pH control

The use of the vapor-fed anode chamber combined with the zero-gap electrode spacing successfully maintained the catholyte pH in the range of 6.6–7.2 under all test conditions, and thus no pH adjustments were needed (Fig. 3). To confirm the stability of this near-neutral pH condition over a longer period of time, the cycle length was extended to 6 days in an additional batch cycle, and the catholyte pH did not increase (7.0 ± 0.0). Conventional MES systems using a membrane between the electrodes require additional pH control through addition of an acid to the catholyte (Liu et al., 2017; van Eerten-Jansen et al., 2015) or a specialized CO_2 delivery system to buffer the pH of the biocathode (Bian et al., 2021). Otherwise, the catholyte pH will became strongly alkaline (7.7–10.1 depending on the buffer concentration) in these systems (Zhou et al., 2021, 2020). The stable pH of the medium in our system was due to the vapor-fed anode configuration and use of CEM between anode and cathode. The vapor fed to the anode enabled a selective transport of protons from the anode, rather than transport of other ions that would be present in a liquid anolyte such as sodium and potassium. The small spacing between anode and cathode enabled effective transport the protons generated at the anode directly to the biocathode, minimizing local pH changes and reducing mass-transfer limitations. Maintaining a stable pH in the MES cells reduced the voltage required to drive the electrochemical reactions, as a pH gradient will increase the required thermodynamic potential according to the Nernst equation.

3.3. VFA production and cathodic recovery

There was no measurable VFA production in the initial cycles (2–8), but low concentrations of acetate and propionate were detected in cycle 10 (Fig. 4A). The concentrations of acetate and propionate subsequently increased rapidly and reached their maximum production rates with 940 ± 250 mmol/m^2-d in cycle 22 for acetate, and 180 ± 30 mmol/m^2-d in cycle 20 for propionate. Formate was detected only in cycle 20, with a production rate of 200 ± 120 mmol/m^2-d. The production of VFAs and methane show that there was a competition for the production of these chemicals, and that the production of VFAs took a longer period of time to evolve. The production rates observed in our systems were much higher than previously reported values (63 mmol formate /m^2-d, 59 mmol acetate/m^2-d (Yu et al., 2017), 607 mmol acetate/m^2-d (Rojas et al., 2018a). Acetate is one of the major products from MES systems and propionate can be produced at more negative cathodic potential than acetate because more electrons are needed (14 electrons for propionate and 8 electrons for acetate). Although we could not measure cathodic potential, there are several MES systems where propionate was produced as one of the final products along with acetate, butyrate, and other chemicals in the catholyte at a cathodic potential of −0.6 to –1.0 V vs. standard hydrogen electrode (Das et al., 2018, 2020; S. Das and Ghangrekar, 2021; Modestra et al., 2015). Hydrogen gas was first detected when the applied potential was increased from 2.8 V to 3.1 V, indicating that net hydrogen evolution occurred due to insufficient uptake by microorganisms on the cathode.

The overall cathodic recovery calculated based on methane, hydrogen, and VFA production, was higher than 100% with production of VFAs (Fig. 4B). Cathodic recoveries of >100% have been previously reported in several MES studies (Siegert et al., 2014; Zhen et al., 2016),

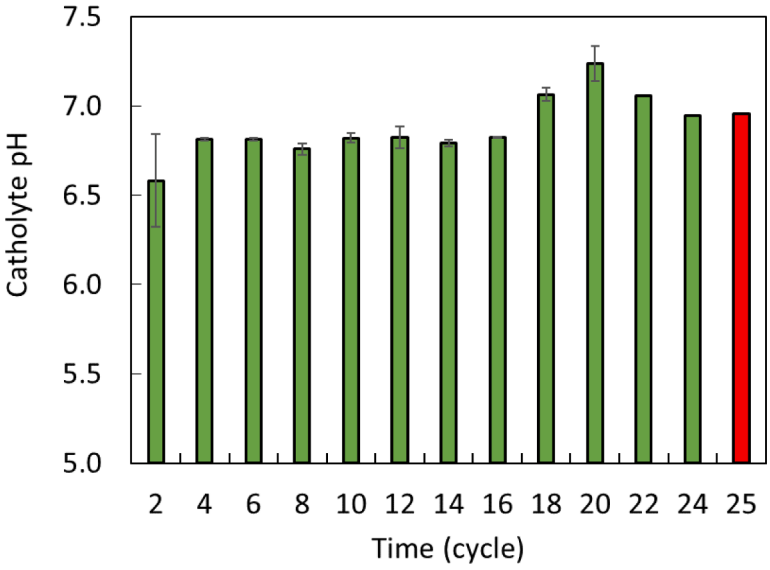

Fig. 3. Catholyte pH at the end of each cycle. The MES systems were operated for a longer period (6 days) for the 25th cycle (indicated with red color).

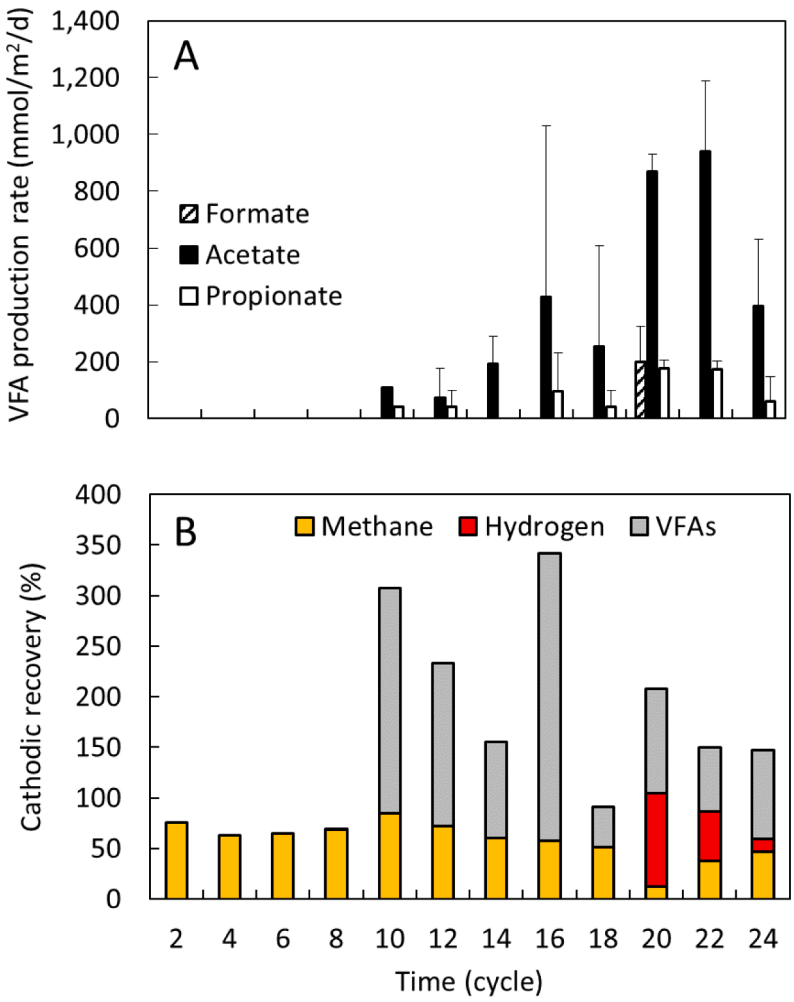

Fig. 4. (A) volatile fatty acid (VFA) production rate and (B) total cathodic recovery based on both biogas and liquid chemical productions at the end of each cycle.

with a very high value of ~1200% obtained when carbon black was used as a cathode material in two-chamber MMCs (Siegert et al., 2014). In that study, the authors suggested that high columbic efficiency might be due to a cathode corrosion via $2C^0 + 3H_2O \rightarrow CH_4 + HCO_3^- + H^+$ ($\Delta G^0 =$ 17 kJ/mol) as there was no methane production from open-circuit controls, and methane production was greater than abiotic H_2 production in controls with an applied voltage (Siegert et al., 2014). Thus, it seems likely here that cathode corrosion contributed to providing additional electrons to be used for either VFA or methane production at least in part, but there has been no well-known mechanism to explain this high cathodic recovery. The use of radio-labelled CO_2 could be used as a way to investigate the source of the methane and VFAs produced in these systems in future MES studies.

To confirm that current and chemical production were not due only to abiotic reactions the cathode was replaced with a new cathode (no biofilm) and 2.8 V was applied (Fig. S4). When E_{ap} of 2.8 V was applied for each cycle, the abiotic system had a current density of 1.5 ± 0.2 A/m^2, indicating that abiotic reactions did contribute to current. However, this current was only 20% of the average current produced in the MES system of 8.2 ± 0.1 A/m^2.

Methanogens are obligate anaerobes, and therefore an oxygen scavenger (100 mg/L of L-cysteine HCl) was added to the catholyte in the last batch cycle to see if any small amounts of oxygen leaking into the system might adversely impact chemical production (Fig. S5) (Wang et al., 2021). The current density was immediately increased from 4.4 A/m^2 to 6.2 A/m^{2}after L-cysteine was added, suggesting that the oxygen scavenging was beneficial to microorganisms in the cathode biofilm. After 1 h of operation, the catholyte was replaced with a fresh medium lacking L-cystine, and the higher current density was maintained during rest of cell operation time. Given that the conductivity of catholyte was not appreciably increased by the addition of L-cysteine addition (from 8.6 to 9.1), this suggests that the condition of the cathode biofilm once restored by the anoxic conditions could be maintained over time. Further studies on the effect of oxygen scavengers on system performance therefore are warranted as a method of improving system stability and performance.

3.4. Cathode biofilm community structure

The biomass samples taken from the cathode of each MES system were analyzed for 16S rRNA to investigate active microbial community. A total of 187,687 of non-chimeric, quality-filtered reads were obtained from two samples and they were clustered into 101 OTUs at 97% identity. The most abundant 10 OTUs in each sample were shown in a heatmap with their relative abundance and taxonomic classification at the genus and phylum level (Table 1). The most abundantly enriched OTU (OTU 1; 35.7%) belonged to the genus *Methanobrevibacter*, which is a well-known hydrogenotrophic methanogen in anaerobic digestion (AD) (Yang et al., 2019). Many previous MES studies have shown that the genus *Methanobacterium* has had the highest relative abundance in the cathode biofilms at lower current densities (Bian et al., 2021; Cheng et al., 2009; Marshall et al., 2012; Ragab et al., 2020; Siegert et al., 2015a). In addition, this genus was abundant in studies where MECs were used in AD systems (Baek et al., 2021; Cai et al., 2016). Both

Table 1
Heatmap of the relative abundance of the top 10 OTUs of each cathode biofilm of MES systems and average values of duplicates at the genus, family, and phylum level with the corresponding specific OTU.

OTU	Phylum	Family	Genus	MES1 (%)	MES2 (%)	AVG (%)
OTU 1	*Euryarchaeota*	*Methanobacteriaceae*	*Methanobrevibacter*	32.5	38.8	35.7
OTU 2	*Firmicutes*	*Clostridiaceae 1*	*Clostridium sensu stricto 1*	12.4	9.4	10.9
OTU 3	*Firmicutes*	*Eubacteriaceae*	*Eubacterium*	12.7	3.6	8.2
OTU 4	*Bacteroidetes*	*Rikenellaceae*	–	7.0	9.3	8.1
OTU 5	*Proteobacteria*	*Rhodocyclaceae*	*Azospira*	4.0	12.1	8.0
OTU 6	*Proteobacteria*	*Pseudomonadaceae*	*Pseudomonas*	6.5	3.5	5.0
OTU 7	*Proteobacteria*	*Burkholderiaceae*	*Alcaligenes*	4.1	3.6	3.8
OTU 8	*Actinobacteria*	*Nocardiaceae*	*Gordonia*	1.6	2.6	2.1
OTU 9	*Firmicutes*	*Lachnospiraceae*	*Tyzzerella*	1.8	1.7	1.7
OTU 10	*Euryarchaeota*	*Methanobacteriaceae*	*Methanobrevibacter*	2.0	1.0	1.5

cathode potentials and current densities can impact the abundance of different methanogens. The relative abundance of *Methanobacterium* and *Methanobrevibacter*, which belong to the same family of *Methanobacteraceae,* was found to be impacted by cathode potentials set at the start of an MES experiment (Li et al., 2020). At startup using cathode potentials of –0.7, –0.8, and –0.9 V produced an archaeal community almost exclusively dominated by *Methanobacterium*, while at more negative startup cathode potentials, the relative abundance of *Methanobrevibacter* increased to 9% (at –1.0 V) and then 74% (at –1.1 V). The authors proposed that the enrichment of *Methanobrevibacter* at more negative cathode potentials was possibly because they have higher H_2 thresholds (2.0–5.8 Pa) than those of *Methanobacterium* (< 2.0 Pa) (Kim, 2012). In another study, *Methanobrevibacter* had a much higher relative abundance (89–99%) than *Methanobacterium* with a higher current density and H_2 production, while its abundance decreased to 27% with a lower H_2 production (Werner et al., 2016). Similarly, *Methanobrevibacter* predominated (86–100%) on biocathodes using platinum-coated cathode materials, while the MES systems with other cathode materials (e.g., plain carbon, Ni, magnetite, steel, ferrihydrite, FeS, and MoS_2) yielded biofilms enriched with *Methanobacterium* (Siegert et al., 2015b). Given that platinum is primarily used as a cathode catalyst for an efficient H_2 production to reduce the high overpotential for proton reduction (Chae et al., 2009), the emergence of active H_2 production at the cathode in the later batch cycles might help to explain the predominance of *Methanobrevibacter*.

For the bacterial community, OTU 2 belonging to the genus *Clostridium sensu stricto 1* had the highest relative abundance, although it was only 10.9%. The dominance of *Clostridium* on the cathode in MES studies has have been previously reported, although at higher relative abundances of 40.4% of the total bacterial community (Vidales et al., 2021). *Clostridium* are acetogenic bacteria which have been shown to convert CO_2 to acetate on electrodes (Logan et al., 2019; Nevin et al., 2011), and their presence on the cathode here is consistent with the observation of acetate production in the later cycles (Fig. 4). OTUs 3 and 5 belonged to genera *Eubacterium* and *Azospira* and showed distinct relative abundances between duplicate biocathodes. Members of the genus *Eubacterium* are known as chemolithoautotrophs and have been found in biofilms on electrodes that were switched to operate as cathodes after functioning as anodes in sediment-type MFCs (Pisciotta et al., 2012). *Azospira* is known to perform heterotrophic denitrification, it was recently found to be abundant on the biocathode in a nitrogen-removing bioelectrochemical system (Sun et al., 2019), and this genus is known to use acetate as a carbon source under both anaerobic and aerobic conditions (Nam et al., 2016). *Pseudomonas*, affiliated with OTU 6, has been reported as a putative electrotroph that could uptake electrons from the cathode and survive on its surface (Li et al., 2021; Roy et al., 2021; Vidales et al., 2021). *Alcaligenes* were previously found from the anode biofilm but not from the cathode biofilm, suggesting their minor role at the cathode in the MES process (Vidales et al., 2021). The appearance of the genus *Gordonia* might be due to possible oxygen leakage into the systems suggested by the result of L-cystein test, given that this genus is aerobic (Arenskötter et al., 2004). The use of pure cultures of these or other microorganisms in the cathode chamber could lead to more effective controls on the specific chemical products. Propionate production from current density in bioelectrochemical systems is known to be performed by propionate-producing bacteria such as members belonging to the genus *Propionibacterium* (Emde and Schink, 1990; Rabaey and Rozendal, 2010). Although no species affiliated to *Propionibacterium* were detected in our cathode biofilms, two OTUs in our libraries were affiliated to the family *Propionibacteriaceae* where the genus *Propionibacterium* belong to (both OTUs were not revealed at the genus level). Since the relative abundances of both OTUs were considerable (0.3 and 0.2%, each; data not shown), they might be responsible for propionate production at the cathode.

3.5. Comparison of methane production rates to previous studies

The methane production rate obtained here of 2.9 ± 1.2 L/L-d (platinized titanium felt anode) (Fig. 2) was larger than that in most previous reports, and the applied voltage (E_{ap} = 3.1 V) was also much lower than in these previous studies (when reported). For example, in a study by Zhou et al. (2021), the methane production rate was 1.6 L/L-d (our calculation based on 202 L/m^2-*d* and the reported cathode area), with an applied voltage of E_{ap} = 5.5 V compared to 3.1 V here (Zhou et al., 2021). The use of set cathode potentials could be expected to improve methane production rates since the anode potential will vary to enable the set current. However, the use of very high cell voltages to produce this current would result in a reduction of energy efficiency. In a study by Kracke et al. (2020), the methane production rate was indicated to be a record high of 1.4 L/L-d at a set current density of 10 A/m^2 (Kracke et al., 2020). However, the cell voltage used to obtain this result was not reported. Important differences between their study and ours includes their use of NiMo-catalyzed cathode, a two-bottle architecture, and pure cultures of the hydrogenotrophic methanogen (*Methanococcus maripaludis*). Here we used no cathode catalyst and only anaerobic sludge as the inoculum in our reactor which had a much different architecture. A higher volumetric methane production rate of 4.3 L/L-d was obtained by Zhou et al. (2020) with a set current density of 35 A/m^2 and cathodes made of granular activated carbon (GAC) (Zhou et al., 2020). However, the methane production rate was only 1.0 L/L-d at the same current density of 10 A/m^2 used by Kracke et al. (2020), and the cell voltage needed to produce this current was not reported. Assuming a linear relationship between current and methane production, this suggests the system used by Zhou et al. (2020) would have produced a smaller rate of 2.1 L/L-d at the same current density as that used here (17.4 A/m^2). The lack of data on cell voltages does not allow for direct comparisons of methane production relative to energy input.

The very low ohmic resistance of the vapor-fed, zero gap electrode system used here (2.4 ± 0.5 mΩ m^2) suggests that the methane production rates were superior to previous studies based on the energy needed to be added to achieve these high volumetric methane production rates. The ohmic resistance measured in our study by the current

interrupt method was 2.4 ± 0.5 mΩ m^2, which was much lower than that of conventional MECs made with cube-cell or tubular design (20–25 mΩ m^2) (Cario et al., 2019; Guo et al., 2017). In addition, the measured resistance showed similar values to those obtained for zero-gap MECs (2.2 mΩ m^2) (Rossi et al., 2021a), indicating that no space between anode and cathode (i.e., the electrodes pressed against to the ion exchange membrane) was a key to reduce the overall resistance and thus improve electrochemical performance.

Although the experiment here was conducted in a small reactor size, a novel design developed here could be up scaled for future applications. There are several advantages of this reactor design for up-scaling compared to the conventional MES systems using a liquid anolyte. First, it is not necessary to provide electrolyte into the anode chamber, so we can reduce the energy and cost for preparing and pumping buffer solutions. Second, there is lower possibility of unwanted reactions on the anode, such as chemical precipitation, catalyst leaching and dissolution, and oxidation of chemical species because the anode does not directly contact with the liquid buffer (Rossi et al., 2021a). In addition, an acidic anolyte and basic catholyte are not produced in this configuration that would require further treatment. In contrast, there are some possible challenges when this MES configuration becomes bigger. Since the catholyte flowed through the carbon felt in the current reactor design and thus there is always the potential for electrode clogging over time (Zhai and Dong, 2022).

4. Conclusions

A newly designed zero-gap and vapor-fed MES reactor enabled one of the highest methane production rates of 2.9 ± 1.2 L/L-d at an $E_{ap} = 3.1$ V using electrodes as an electron donor and CO_2 as the carbon source. The vapor-fed anode pressed against a CEM enabled selective transport of protons to the cathode, as demonstrated by a catholyte pH that was maintained at a circumneutral pH of 6.6–7.2 over time. The zero-gap configuration enabled a low ohmic resistance of 2.4 ± 0.5 mΩ m^2, which is much lower than previous systems. Over multiple cycles, VFAs were also produced showing that competition for the electrons donated by the cathode to the biofilm resulted in production of multiple chemical products. The cathode biofilm was mainly comprised of the hydrogenotrophic methanogen *Methanobrevibacter* and the acetogenic bacterium *Clostridium sensu stricto 1* together, suggesting their roles in producing both methane and VFAs from CO_2 as final products. Some hydrogen was produced along with the other chemical products, suggesting that the cathode design could be improved to avoid production of unwanted chemical products in these systems. The novel reactor design here could lead to efficient chemical production from electrical current compared to previous systems.

Declaration of Competing Interest

The authors declare that they have no known competing financial interests or personal relationships that could have appeared to influence the work reported in this paper.

Acknowledgements

This research was funded by the Stan and Flora Kappe endowment and other funds through The Pennsylvania State University.

Supplementary materials

Supplementary material associated with this article can be found, in the online version, at doi:10.1016/j.watres.2022.118597.

References

Alqahtani, M.F., Katuri, K.P., Bajracharya, S., Yu, Y., Lai, Z., Saikaly, P.E., 2018. Porous hollow fiber nickel electrodes for effective supply and reduction of carbon dioxide to methane through microbial electrosynthesis. Adv. Func. Mat. 28 (43), 1804860.
Arenskötter, M., Bröker, D., Steinbüchel, A., 2004. Biology of the metabolically diverse genus Gordonia. Appl. Environ. Microbiol. 70 (6), 3195–3204.
Aryal, N., Tremblay, P.-L., Lizak, D.M., Zhang, T., 2017. Performance of different *Sporomusa* species for the microbial electrosynthesis of acetate from carbon dioxide. Bioresour. Technol. 233, 184–190.
Baek, G., Saikaly, P.E., Logan, B.E., 2021. Addition of a carbon fiber brush improves anaerobic digestion compared to external voltage application. Water Res 188, 116575.
Baek, G., Shi, L., Rossi, R., Logan, B.E., 2022. Using copper-based biocathodes to improve carbon dioxide conversion efficiency into methane in microbial methanogenesis cells. Chem. Eng. J., 135076
Bajracharya, S., Srikanth, S., Mohanakrishna, G., Zacharia, R., Strik, D.P., Pant, D., 2017. Biotransformation of carbon dioxide in bioelectrochemical systems: state of the art and future prospects. J. Power Sour. 356, 256–273.
Batlle-Vilanova, P., Puig, S., Gonzalez-Olmos, R., Balaguer, M.D., Colprim, J., 2016. Continuous acetate production through microbial electrosynthesis from CO_2 with microbial mixed culture. J. Chem. Technol. Biotechnol. 91 (4), 921–927.
Beese-Vasbender, P.F., Grote, J.-.P., Garrelfs, J., Stratmann, M., Mayrhofer, K.J., 2015. Selective microbial electrosynthesis of methane by a pure culture of a marine lithoautotrophic archaeon. Bioelectrochemistry 102, 50–55.
Bian, B., Xu, J., Katuri, K.P., Saikaly, P.E., 2021. Resistance assessment of microbial electrosynthesis for biochemical production to changes in delivery methods and CO_2 flow rates. Bioresour. Technol. 319, 124177.
Cai, W., Liu, W., Yang, C., Wang, L., Liang, B., Thangavel, S., Guo, Z., Wang, A., 2016. Biocathodic methanogenic community in an integrated anaerobic digestion and microbial electrolysis system for enhancement of methane production from waste sludge. ACS Sust. Chem. Eng. 4 (9), 4913–4921.
Cario, B.P., Rossi, R., Kim, K.-.Y., Logan, B.E., 2019. Applying the electrode potential slope method as a tool to quantitatively evaluate the performance of individual microbial electrolysis cell components. Bioresour. Technol. 287, 121418.
Chae, K.-.J., Choi, M.-.J., Kim, K.-.Y., Ajayi, F.F., Chang, I.-.S., Kim, I.S., 2009. A solar-powered microbial electrolysis cell with a platinum catalyst-free cathode to produce hydrogen. Environ. Sci. Technol. 43 (24), 9525–9530.
Cheng, S., Xing, D., Call, D.F., Logan, B.E., 2009. Direct biological conversion of electrical current into methane by electromethanogenesis. Environ. Sci. Technol. 43 (10), 3953–3958.
Dargahi, M., Hosseinidoust, Z., Tufenkji, N., Omanovic, S., 2014. Investigating electrochemical removal of bacterial biofilms from stainless steel substrates. Colloid. Surf. B: Biointerfaces 117, 152–157.
Das, S., Chatterjee, P., Ghangrekar, M., 2018. Increasing methane content in biogas and simultaneous value added product recovery using microbial electrosynthesis. Water Sci. Technol. 77 (5), 1293–1302.
Das, S., Das, I., Ghangrekar, M., 2020. Role of applied potential on microbial electrosynthesis of organic compounds through carbon dioxide sequestration. J. Environ. Chem. Eng. 8 (4), 104028.
Das, S., Das, S., Ghangrekar, M., 2021. Application of TiO_2 and Rh as cathode catalyst to boost the microbial electrosynthesis of organic compounds through CO_2 sequestration. Process Biochem 101, 237–246.
Das, S., Ghangrekar, M., 2021. Performance comparison between batch and continuous mode of operation of microbial electrosynthesis for the production of organic chemicals. J. Appl. Electrochem. 51 (5), 715–725.
Deutzmann, J.S., Spormann, A.M., 2017. Enhanced microbial electrosynthesis by using defined co-cultures. The ISME J 11 (3), 704–714.
Emde, R., Schink, B., 1990. Enhanced propionate formation by *Propionibacterium freudenreichii subsp. freudenreichii* in a three-electrode amperometric culture system. Appl. Environ. Microbiol. 56 (9), 2771–2776.
Fang, W., Zhang, P., Zhang, G., Jin, S., Li, D., Zhang, M., Xu, X., 2014. Effect of alkaline addition on anaerobic sludge digestion with combined pretreatment of alkaline and high pressure homogenization. Bioresour. Technol. 168, 167–172.
Guo, K., Prévoteau, A., Rabaey, K., 2017. A novel tubular microbial electrolysis cell for high rate hydrogen production. J. Power Sour. 356, 484–490.
Jiang, Y., Chu, N., Zhang, W., Ma, J., Zhang, F., Liang, P., Zeng, R.J., 2019a. Zinc: a promising material for electrocatalyst-assisted microbial electrosynthesis of carboxylic acids from carbon dioxide. Water Res 159, 87–94.
Jiang, Y., May, H.D., Lu, L., Liang, P., Huang, X., Ren, Z.J., 2019b. Carbon dioxide and organic waste valorization by microbial electrosynthesis and electro-fermentation. Water Res 149, 42–55.
Jiang, Y., Su, M., Zhang, Y., Zhan, G., Tao, Y., Li, D., 2013. Bioelectrochemical systems for simultaneously production of methane and acetate from carbon dioxide at relatively high rate. Int. J. Hydrogen Energ. 38 (8), 3497–3502.
Jourdin, L., Burdyny, T., 2021. Microbial electrosynthesis: where do we go from here? Trends Biotechnol 39 (4), 359–369.
Karthikeyan, R., Singh, R., Bose, A., 2019. Microbial electron uptake in microbial electrosynthesis: a mini-review. J. Ind. Microbiol. Biotechnol. 46 (9–10), 1419–1426.
Katuri, K.P., Werner, C.M., Jimenez-Sandoval, R.J., Chen, W., Jeon, S., Logan, B.E., Lai, Z., Amy, G.L., Saikaly, P.E., 2014. A novel anaerobic electrochemical membrane bioreactor (AnEMBR) with conductive hollow-fiber membrane for treatment of low-organic strength solutions. Environ. Sci. Technol. 48 (21), 12833–12841.
Kim, C.C.-h., 2012. Identification of Rumen methanogens, Characterization of Substrate Requirements and Measurement of Hydrogen thresholds: a Thesis Presented in

Partial Fulfilment of the Requirements For the Degree of Master's in Microbiology. Massey University.
Kracke, F., Deutzmann, J.S., Gu, W., Spormann, A.M., 2020. In situ electrochemical H_2 production for efficient and stable power-to-gas electromethanogenesis. Green Chem 22 (18), 6194–6203.
Kracke, F., Wong, A.B., Maegaard, K., Deutzmann, J.S., Hubert, M.A., Hahn, C., Jaramillo, T.F., Spormann, A.M., 2019. Robust and biocompatible catalysts for efficient hydrogen-driven microbial electrosynthesis. Commun. Chem. 2 (1), 1–9.
Lavender, M.B., Pang, S., Liu, D., Jourdin, L., Ter Heijne, A., 2022. Reduced overpotential of methane-producing biocathodes: effect of current and electrode storage capacity. Bioresour. Technol. 347, 126650.
Li, J., Li, Z., Xiao, S., Fu, Q., Kobayashi, H., Zhang, L., Liao, Q., Zhu, X., 2020. Startup cathode potentials determine electron transfer behaviours of biocathodes catalysing CO_2 reduction to CH_4 in microbial electrosynthesis. J. CO_2 Util 35, 169–175.
Li, X.-.M., Ding, L.-.J., Zhu, D., Zhu, Y.-.G., 2021. Long-term fertilization shapes the putative electrotrophic microbial community in paddy soils revealed by microbial electrosynthesis systems. Environ. Sci. Technol. 55 (5), 3430–3441.
Li, X., Angelidaki, I., Zhang, Y., 2018. Salinity-gradient energy driven microbial electrosynthesis of value-added chemicals from CO_2 reduction. Water Res 142, 396–404.
Lienemann, M., Deutzmann, J.S., Milton, R.D., Sahin, M., Spormann, A.M., 2018. Mediator-free enzymatic electrosynthesis of formate by the *Methanococcus maripaludis* heterodisulfide reductase supercomplex. Bioresour. Technol. 254, 278–283.
Liu, C., Xiao, J., Li, H., Chen, Q., Sun, D., Cheng, X., Li, P., Dang, Y., Smith, J.A., Holmes, D.E., 2021. High efficiency in-situ biogas upgrading in a bioelectrochemical system with low energy input. Water Res 197, 117055.
Liu, D., Zheng, T., Buisman, C., Ter Heijne, A., 2017. Heat-treated stainless steel felt as a new cathode material in a methane-producing bioelectrochemical system. ACS Sust. Chem. Eng. 5 (12), 11346–11353.
Logan, B.E., Rossi, R., Ragab, A., Saikaly, P.E., 2019. Electroactive microorganisms in bioelectrochemical systems. Nat. Rev. Microbiol. 17 (5), 307–319.
Logan, B.E., Wallack, M.J., Kim, K.-.Y., He, W., Feng, Y., Saikaly, P.E., 2015. Assessment of microbial fuel cell configurations and power densities. Environ. Sci. Technol. Lett. 2 (8), 206–214.
Marshall, C.W., Ross, D.E., Fichot, E.B., Norman, R.S., May, H.D., 2012. Electrosynthesis of commodity chemicals by an autotrophic microbial community. Appl. Environ. Microbiol. 78 (23), 8412–8420.
Mayer, F., Enzmann, F., Lopez, A.M., Holtmann, D., 2019. Performance of different methanogenic species for the microbial electrosynthesis of methane from carbon dioxide. Bioresour. Technol. 289, 121706.
Modestra, J.A., Navaneeth, B., Mohan, S.V., 2015. Bio-electrocatalytic reduction of CO_2: enrichment of homoacetogens and pH optimization towards enhancement of carboxylic acids biosynthesis. J. CO_2 Util 10, 78–87.
Nam, J.-.H., Ventura, J.-R.S., Yeom, I.T., Lee, Y., Jahng, D., 2016. A novel perchlorate- and nitrate-reducing bacterium, *Azospira sp*. PMJ. Appl. Microbiol. Biotechnol. 100 (13), 6055–6068.
Nevin, K.P., Hensley, S.A., Franks, A.E., Summers, Z.M., Ou, J., Woodard, T.L., Snoeyenbos-West, O.L., Lovley, D.R., 2011. Electrosynthesis of organic compounds from carbon dioxide is catalyzed by a diversity of acetogenic microorganisms. Appl. Environ. Microbiol. 77 (9), 2882–2886.
Pisciotta, J.M., Zaybak, Z., Call, D.F., Nam, J.-.Y., Logan, B.E., 2012. Enrichment of microbial electrolysis cell biocathodes from sediment microbial fuel cell bioanodes. Appl. Environ. Microbiol. 78 (15), 5212–5219.
Prévoteau, A., Carvajal-Arroyo, J.M., Ganigué, R., Rabaey, K., 2020. Microbial electrosynthesis from CO_2: forever a promise? Curr. Opin. Biotechnol. 62, 48–57.
Rabaey, K., Rozendal, R.A., 2010. Microbial electrosynthesis—Revisiting the electrical route for microbial production. Nat. Rev. Microbiol. 8 (10), 706–716.
Ragab, A., Katuri, K.P., Ali, M., Saikaly, P.E., 2019. Evidence of spatial homogeneity in an electromethanogenic cathodic microbial community. Front. Microbiol. 10, 1747.
Ragab, A., Shaw, D.R., Katuri, K.P., Saikaly, P.E., 2020. Effects of set cathode potentials on microbial electrosynthesis system performance and biocathode methanogen function at a metatranscriptional level. Sci. Rep. 10 (1), 1–15.
Rojas, M.d.P.A., Mateos, R., Sotres, A., Zaiat, M., Gonzalez, E.R., Escapa, A., De Wever, H., Pant, D., 2018a. Microbial electrosynthesis (MES) from CO_2 is resilient to fluctuations in renewable energy supply. Energ. Convers. Manage. 177, 272–279.
Rojas, M.d.P.A., Zaiat, M., Gonzalez, E.R., De Wever, H., Pant, D., 2018b. Effect of the electric supply interruption on a microbial electrosynthesis system converting inorganic carbon into acetate. Bioresour. Technol. 266, 203–210.
Rossi, R., Baek, G., Logan, B.E., 2021a. Vapor-fed cathode microbial electrolysis cells with closely spaced electrodes enables greatly improved performance. Environ. Sci. Technol.
Rossi, R., Baek, G., Saikaly, P.E., Logan, B.E., 2021b. Continuous flow microbial flow cell with an anion exchange membrane for treating low conductivity and poorly buffered wastewater. ACS Sust. Chem. Eng. 9 (7), 2946–2954.
Rossi, R., Logan, B.E., 2020. Unraveling the contributions of internal resistance components in two-chamber microbial fuel cells using the electrode potential slope analysis. Electrochim. Acta 348, 136291.
Roy, M., Yadav, R., Chiranjeevi, P., Patil, S.A., 2021. Direct utilization of industrial carbon dioxide with low impurities for acetate production via microbial electrosynthesis. Bioresour. Technol. 320, 124289.
Rozendal, R.A., Hamelers, H.V., Buisman, C.J., 2006. Effects of membrane cation transport on pH and microbial fuel cell performance. Environ. Sci. Technol. 40 (17), 5206–5211.
Siegert, M., Li, X.-.F., Yates, M.D., Logan, B.E., 2015a. The presence of hydrogenotrophic methanogens in the inoculum improves methane gas production in microbial electrolysis cells. Front. Microbiol. 5, 778.
Siegert, M., Yates, M.D., Call, D.F., Zhu, X., Spormann, A., Logan, B.E., 2014. Comparison of nonprecious metal cathode materials for methane production by electromethanogenesis. ACS Sust. Chem. Eng. 2 (4), 910–917.
Siegert, M., Yates, M.D., Spormann, A.M., Logan, B.E., 2015b. *Methanobacterium* dominates biocathodic archaeal communities in methanogenic microbial electrolysis cells. ACS Sust. Chem. Eng. 3 (7), 1668–1676.
Sun, J., Xu, W., Cai, B., Huang, G., Zhang, H., Zhang, Y., Yuan, Y., Chang, K., Chen, K., Peng, Y., 2019. High-concentration nitrogen removal coupling with bioelectric power generation by a self-sustaining algal-bacterial biocathode photo-bioelectrochemical system under daily light/dark cycle. Chemosphere 222, 797–809.
van Eerten-Jansen, M.C., Jansen, N.C., Plugge, C.M., de Wilde, V., Buisman, C.J., ter Heijne, A., 2015. Analysis of the mechanisms of bioelectrochemical methane production by mixed cultures. J. Chem. Technol. Biotechnol. 90 (5), 963–970.
Vidales, A.G., Bruant, G., Omanovic, S., Tartakovsky, B., 2021. Carbon dioxide conversion to C1-C2 compounds in a microbial electrosynthesis cell with in situ electrodeposition of nickel and iron. Electrochim. Acta 383, 138349.
Wang, Y., Xi, B., Jia, X., Li, M., Qi, X., Xu, P., Zhao, Y., Ye, M., Hao, Y., 2021. Characterization of hydrogen production and microbial community shifts in microbial electrolysis cells with L-cysteine. Sci. Tot. Environ. 760, 143353.
Werner, C.M., Katuri, K.P., Hari, A.R., Chen, W., Lai, Z., Logan, B.E., Amy, G.L., Saikaly, P.E., 2016. Graphene-coated hollow fiber membrane as the cathode in anaerobic electrochemical membrane bioreactors–Effect of configuration and applied voltage on performance and membrane fouling. Environ. Sci. Technol. 50 (8), 4439–4447.
Wood, J.C., Grové, J., Marcellin, E., Heffernan, J.K., Hu, S., Yuan, Z., Virdis, B., 2021. Strategies to improve viability of a circular carbon bioeconomy-A techno-economic review of microbial electrosynthesis and gas fermentation. Water Res 201, 117306.
Yang, Z., Wang, W., Liu, C., Zhang, R., Liu, G., 2019. Mitigation of ammonia inhibition through bioaugmentation with different microorganisms during anaerobic digestion: selection of strains and reactor performance evaluation. Water Res 155, 214–224.
Yi, Y., Weinberg, G., Prenzel, M., Greiner, M., Heumann, S., Becker, S., Schlögl, R., 2017. Electrochemical corrosion of a glassy carbon electrode. Catal. Today 295, 32–40.
Yu, L., Yuan, Y., Tang, J., Zhou, S., 2017. Thermophilic *Moorella thermoautotrophica*-immobilized cathode enhanced microbial electrosynthesis of acetate and formate from CO_2. Bioelectrochemistry 117, 23–28.
Zhai, J., Dong, S., 2022. Recent advances in microbial fuel cell-based toxicity biosensors: strategies for enhanced toxicity response. Curr. Opin. Electrochem., 100975
Zhen, G., Lu, X., Kobayashi, T., Kumar, G., Xu, K., 2016. Promoted electromethanosynthesis in a two-chamber microbial electrolysis cells (MECs) containing a hybrid biocathode covered with graphite felt (GF). Chem. Eng. J. 284, 1146–1155.
Zhou, H., Xing, D., Xu, M., Su, Y., Ma, J., Angelidaki, I., Zhang, Y., 2021. Optimization of a newly developed electromethanogenesis for the highest record of methane production. J. Hazard. Mat. 407, 124363.
Zhou, H., Xing, D., Xu, M., Su, Y., Zhang, Y., 2020. Biogas upgrading and energy storage via electromethanogenesis using intact anaerobic granular sludge as biocathode. Appl. Energ. 269, 115101.